*Journal of Electromyography and Kinesiology*
Vol. 1, No. 4, 263–269


# Technique for Interpretation of Electromyography for Concentric and Eccentric Contractions in Gait

David A. Winter and Stephen H. Scott

*Department of Kinesiology, University of Waterloo, Waterloo, Ontario, Canada*

**Summary:** We present a technique to combine muscle shortening and lengthening velocity information with electromyographic (EMG) profiles during gait. A biomechanical model was developed so that each muscle's length could be readily calculated over time as a function of angles of the joints it crossed. The velocity of shortening and lengthening of the muscle fiber was then calculated, and with computer graphics this information was overlaid on the EMG profiles. Thus, researchers and clinicians were not only able to interpret the processed EMG signal as level of activity (tension) but also to gain insight as to the muscles' role as generators (muscle shortening) or absorbers (muscle lengthening) of energy. Six common muscles are documented, using database profiles; soleus (SOL), medial gastrocnemius (MG), tibialis anterior (TA), vastus lateralis (VL), rectus femoris (RF), and semitendinosus (ST). The protocol thus demonstrates a relatively simple technique for calculating muscle fiber velocity and for combining that velocity information with EMG activity profiles. **Key Words:** Gait—Electromyography—Concentric—Eccentric.

Electromyographic (EMG) signals in raw or processed form are routinely used in assessment of muscle activation during gait. Processed versions of the raw EMG signals such as the linear envelope have been interpreted as estimates of the relative tension within the muscle (7,13). These EMG profiles provide researchers with information about the time-course of activity of the muscle but do not reflect tension-velocity changes and the energy generation/absorption role of each muscle over the gait cycle. Frequently, joint angles are measured simultaneously with the EMG signal; this, combined with our knowledge of anatomy, offers the potential for estimating muscle length as a function of joint angles (2). We report an analytical technique for six major lower limb muscles that allows muscle length and therefore muscle velocity to be calculated from joint angle data. Computer graphic techniques are used to overlay this information on the EMG profiles to allow more meaningful interpretation of each muscle's function in gait. With this technique, researchers and clinicians will be able to assess the activity level of each muscle and simultaneously evaluate the role of the muscle as a generator (shortening velocity) or as an absorber (lengthening velocity) of energy.

## THEORY

Researchers and clinical assessors can process the raw EMG signals from either surface or indwelling electrodes in many ways to obtain an analog signal from which to interpret movement. The choice of surface versus indwelling electrodes is a subject of continuing argument. However, for superficial muscles, several advantages of surface electrodes have been demonstrated. The obvious ease of application of surface electrodes is evident, and their reliability is greatly superior (4,5). No

Accepted April 17, 1991.
Address correspondence and reprint requests to Dr. D. A. Winter at Department of Kinesiology, University of Waterloo, Waterloo, Ontario N2L 3G1, Canada.

valid study has yet been reported to demonstrate the superiority of either surface or indwelling electrodes in terms of cross-talk. Processing the EMG signals as a linear envelope (LE) has the strongest physiologic basis, and arguments for such use have been presented by many researchers 1,3,7,12,14). A number of other processing schemes have been introduced (4) without presenting any physiologic basis. Figure 1 shows the similarity of a suitably chosen LE profile and a muscle tension waveform. The LE processing involved has a transfer characteristic similar to that relating the EMG signal to muscle twitch. The twitch waveform is the impulse response of single motor unit (MU) in which the motor unit action potential (MUAP) can be considered an impulselike neurologic input. The shape of the twitch has been shown to have the frequency characteristics of a second-order critically damped system (6). Thus, the frequency characteristics of a critically damped low-pass filter used in the LE processing could be chosen to mimic the twitch response. As shown in Fig. 1, second-order critically damped filters with cutoff of 1.5–4 Hz mimic twitch times from 106 to 40 ms, respectively. The input of the filter is the full-wave-rectified EMG signal, which is a summation of all detected MUAPs, whereas the output of the filter mimics the summation of all twitch waveforms and therefore can be considered a relative tension waveform for that muscle. With suitable and somewhat complex calibrations (7), the absolute tension in each muscle can be predicted, but such calibrations are too time-consuming and impossible to achieve (because of a loss of voluntary control) in most gait pathologies (7). Nevertheless, we are challenged to derive the most from the LE waveform as a relative tension predictor; we provide additional information regarding the shortening and lengthening velocity of the muscle.

The velocities of six muscles [tibialis anterior (TA), soleus (SOL), medial gastrocnemius (MG), vastus lateralis (VL), rectus femoris (RF), and semitendinosus (ST)] were estimated with a model that calculates muscle/tendon lengths using straight lines (8,10) between muscle origin and insertion (or constraint locations, such as patella). The skeletal model used for anatomic locations of origins, insertions, and constraint locations relative to each joint were derived from a scaled model for adults of the pelvis and lower limbs (10). We assume that the tendons are sufficiently stiff not to lengthen appreciably; thus, the velocity of the origin-to-insertion length was considered equal to the muscle fiber velocity. The fiber velocity in meters per second was then divided by the resting fiber length to yield the velocity in resting lengths per second ($l_0/s$). The resting length of each muscle was the length of the contractile component, which was assumed to be equal to its length when the body was in the anatomic position. The volume of each muscle must remain constant when it shortens and lengthens. Thus, with pennate muscles, the angle of pennation increases when the muscle is shortened and decreases when it is lengthened (9). We also assumed that active muscle and fiber lengths were proportional to body height. Thus, the reporting of fiber velocity in $l_0/s$ was applicable for both adults and children.

The scaled model documented by White et al. (10) was varied at each of the hip, knee, and ankle joints; the muscle length was calculated as a fraction of $l_0$ and yielded a nonlinear relationship between muscle length and joint angles. A third-order regression curve was adequate to relate muscle

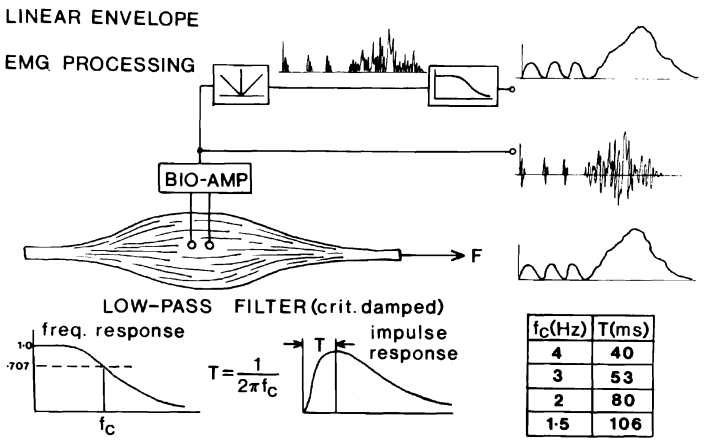


| $f_c$(Hz) | T(ms) |
|---|---|
| 4 | 40 |
| 3 | 53 |
| 2 | 80 |
| 1·5 | 106 |

**FIG. 1.** Relationship between muscle tension waveform and linear envelope (LE) processed electromyogram. The response of the critically damped low-pass filter mimics the twitch; thus, the low-pass filter cut-off frequency can be chosen to model different twitch times as shown.

length to the joint angles. All flexion angles are positive and extension negative. The length of any given muscle, $l_m$, is expressed as:

$$\frac{l_m(t)}{l_0} = 1 + a\theta_1(t) + b\theta_1^2(t) + c\theta_1^3(t) + d\theta_2(t) + e\theta_2^2(t) + f\theta_2^3(t), \quad \text{(Eq. 1)}$$

where $l_m$ is the length change (shortening) of the muscle (origin to insertion); $l_0$ is the resting fiber length of the muscle when the body is in the anatomic position (all θs = 0°); $\theta_1$ is the joint angle for a single joint muscle, in degrees, with flexor being positive; $\theta_2$ is the joint angle for the adjacent joint for a biarticulate muscle with flexor also being positive; and *a–f* are the coefficients as determined by the curve fit. When all joint angles are 0°, $l_m/l_0 = 1$; e.g., for the gastrocnemius muscle, $\theta_1$ refers to the ankle angle and $\theta_2$ refers to the knee angle. If a parallel fiber muscle is being analyzed, the velocity of the muscle fibers (in $l_0/s$) is the same as the velocity of the length of the muscle (assuming no compliance in the tendons).

$$v_f(t) = \frac{d}{dt}\left(\frac{l_m(t)}{l_0}\right). \quad \text{(Eq. 2)}$$

The angle of pennation will change as a result of the length changes as calculated in Eq. 1 and, because the muscle volume remains constant, the pennation angle $\alpha_p$ will change with time (9):

$$\alpha_p(t) = \tan^{-1}\left(\frac{\sin\alpha_0}{\cos\alpha_0 - (1 - lm(t)/l_0)}\right), \quad \text{(Eq. 3)}$$

where $\alpha_0$ is the resting length pennation angle. The active length of the muscle (in $l_0$) is $l_f(t)$:

$$\frac{l_f(t)}{l_0} = \frac{\sin\alpha_0}{\sin\alpha_p(t)}. \quad \text{(Eq. 4)}$$

The velocity of the muscle fibers (in $l_0/s$) is:

$$v_f(t) = \frac{d}{dt}\left(\frac{l_f(t)}{l_0}\right) \quad \text{(Eq. 5)}$$

## METHODS

Because we wished to present a new technique for EMG interpretation, collecting new EMG signal and kinematic data was not critical. Rather than use data from one specific subject, we present data from our database of normal-level walking. Thus, our interpretations of muscle activity related to an average adult gait pattern rather than to specific small differences that would be observed in individual subjects.

The joint angle data were the averaged ankle, knee, and hip angles for 30 adult subjects walking at their natural cadence. Details of the data collection, processing, and analysis were reported previously (7,11,15). Figure 2 shows the ensemble average of the joint angles. The time base was normalized to 100% for the stride period with heel contact (HC) at 0 and 100%. The convention for positive angles is flexion to agree with Eq. 1.

The details of the EMG data collection and processing in LE form was reported previously (7,12,14,16). As indicated in Fig. 1, a midrange cutoff frequency of 3 Hz chosen for low-pass filters, represents an average twitch time of 53 ms. For more accurate profiles, each muscle could be custom-matched to cutoff frequencies related to the twitch times of each muscle. Each subject's EMG

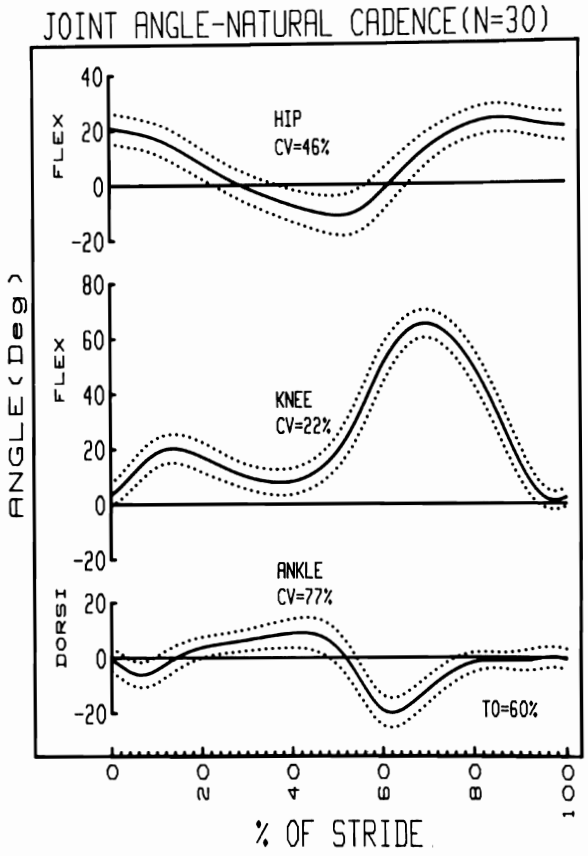


**FIG. 2.** Ensemble average of ankle, knee, and hip joint angles for 30 adult subjects walking at their natural cadence. Convention for polarity of angles is positive for flexion and negative for extension.

TABLE 1. *Coefficients relating muscle length change with joint angle*

| Muscle | *a* | *b* | *c* | *d* | *e* | *f* | $\alpha_0$ |
|---|---|---|---|---|---|---|---|
| TA | $-6.07 \times 10^{-3}$ | $5.86 \times 10^{-5}$ | $4.5 \times 10^{-7}$ | — | — | — | 8 |
| SOL | $2.18 \times 10^{-2}$ | $-8.93 \times 10^{-5}$ | $-9.66 \times 10^{-7}$ | — | — | — | 20 |
| MG | $1.22 \times 10^{-2}$ | $-4.25 \times 10^{-5}$ | $-6.12 \times 10^{-7}$ | $-6.75 \times 10^{-3}$ | $-9.16 \times 10^{-6}$ | $-8.48 \times 10^{-8}$ | 8 |
| VL | $1.06 \times 10^{-2}$ | $-2.28 \times 10^{-5}$ | $-2.28 \times 10^{-7}$ | — | — | — | 13 |
| RF | $1.63 \times 10^{-2}$ | $-1.75 \times 10^{-5}$ | $-4.5 \times 10^{-7}$ | $-1.16 \times 10^{-2}$ | $-6.06 \times 10^{-5}$ | $6.36 \times 10^{-7}$ | 15 |
| ST[a] | $7.3 \times 10^{-3}$ | $1.29 \times 10^{-4}$ | $-8.52 \times 10^{-7}$ | $-1.93 \times 10^{-3}$ | $-9.26 \times 10^{-6}$ | $1.15 \times 10^{-7}$ | 0 |

[a] $\alpha_0$, Pennation angle at $l_0$; TA, tibialis anterior; SOL, soleus; MG, medial gastrocnemius; VL, vastus lateralis; RF, rectus femoris; ST, semitendinosis. *a*, *b*, and *c* coefficients apply to hip angle; *d*, *e*, and *f* coefficients apply to knee angle.

profiles were then normalized to a mean value of 100% over the stride period as detailed previously (14,16) to reduce the variability of intersubject ensemble averages.

Based on the average ankle, knee, and hip joint angles, the change in muscle length was calculated over the stride period from the origin to insertion lengths from the scaled model of the pelvis and lower limbs (10). The joint angle changes and muscle length changes were curve-fitted to a third-order regression Eq. 1 and yielded the coefficients *a–f*, which are shown in Table 1. Using Eq. 2 for parallel fiber muscles or Eq. 3–5 for pennate muscles, we calculated the velocity of shortening and lengthening of the muscle fiber of each muscle. For purposes of clarity with established convention, the polarities were reversed so that shortening velocities were positive and lengthening velocities were negative. The LE profile of each muscle was then shaded according to the polarity and magnitude of the velocity. Based on our observations of the velocity profiles, we chose three velocity ranges for the computer graphics description. Depending on the desired precision of the clinician or researcher, these ranges could be altered or even increased. For near-isometric contractions ($v_f < 0.25\ l_0/s$), there was no shading. For low-velocity shortening ($0.25 < v_f < 1.5\ l_0/s$), the shading was lightly hatched; for higher velocity shortening ($v_f > 1.5\ l_0/s$) the shading was darkly hatched. For lengthening velocities, the velocity limits were the same but the slope of the shading was negative. Positive slope shading thus represents positive muscle work, and negative slope shading indicates negative muscle work.

## RESULTS AND DISCUSSION

We report two representative velocity profiles, one for a single joint muscle and one for a biarticulate muscle, but we describe the polarity and approximate magnitude of the velocities of the other four muscles in conjunction with the LE profiles. The velocity of the SOL (Fig. 3) at HC was positive for the first 8% of stride, indicating a rapid shortening as the foot is lowered rapidly to the floor. Then, during midstance (8–44% of stride), the foot remains flat on the ground and the leg rotates forward, causing SOL to lengthen. Then, during push-off, (44–60% of stride), the tension increases sufficiently to cause rapid plantarflexion and continues to increase until just after toe-off, when maximum plantarflexion is reached at 66% of stride. A very rapid dorsiflexion then occurs, causing SOL to lengthen passively as the foot clears the ground in midswing. The velocity profile of the ST (Fig. 4) is somewhat more difficult to comprehend because of simultaneous changes in the hip and knee joints. Figure 2 shows those joint angle changes: The knee flexes from 0 to 15%, extends from 15 to 40%, flexes from 40 to 70%, and extends again from 70 to 100%; the hip extends from 0 to 50%, flexes from 50 to 90%, and then extends slowly until the next HC. Thus, the positive shortening velocity of ST during all of stance and early swing (0–65%) is mainly due

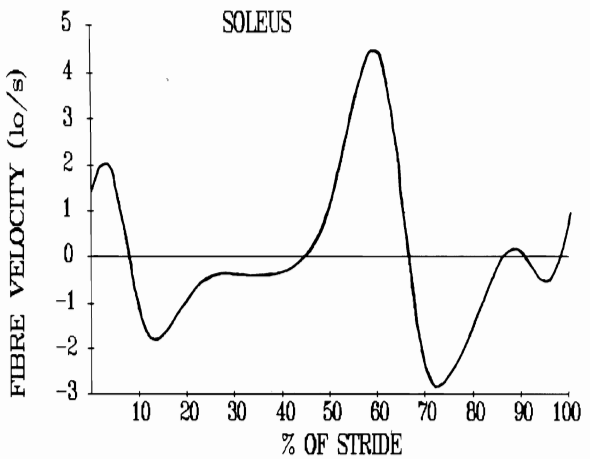


**FIG. 3.** Fiber velocity of soleus muscle over the stride period in $l_0/s$. A positive velocity is shortening; negative velocity is lengthening. Heel contact is at 0 and 100%.

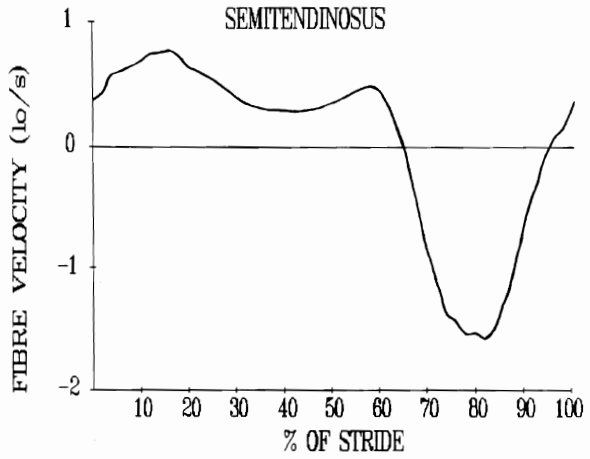


**FIG. 4.** Fiber velocity of semitendinosus muscle over the stride period. This velocity profile, in conjunction with knee and hip angle changes, is described in text.

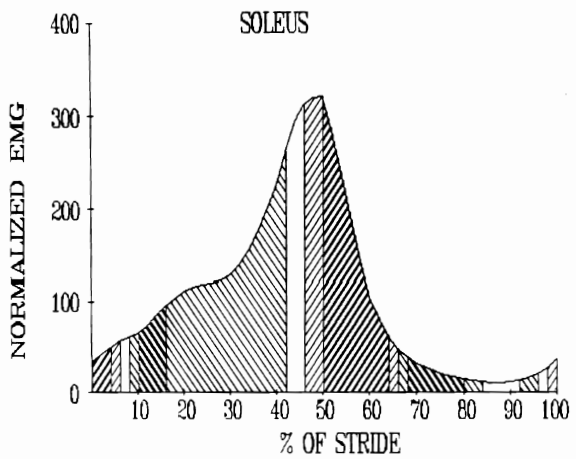


**FIG. 5.** Linear envelope electromyography (EMG) profile of soleus over the stride period. EMG is a normalized intersubject average for each subject's EMG set to 100% before averaging. Positive slope shading indicates positive work (concentric contraction); negative slope shading shows negative work (eccentric contraction); no shading indicates near-isometric. Darker shading indicates higher velocity (>1.5 $l_0$/s), and lighter shading indicates low velocity (0.25 < $v_f$ < 1.5 $l_0$/s).

to the shortening displacement of the origin resulting from the hip extensor velocity during the first 50% of the stride; the shortening displacement of ST at its origin exceeded its lengthening displacement at its insertion when the knee was extending from 15 to 40%. Then from 50 to 65%, the knee is flexing while the hip is also flexing, but the insertion shortening dominates the origin lengthening; thus, ST continues to shorten slowly. During most of the swing (65–95%), ST rapidly lengthens, mainly due to a hip flexor velocity (50–90%) and a knee extensor velocity (70–100%).

The profiles of LE of SOL and MG (Figs. 5 and 6) indicate very similar functional activity. During weight acceptance (0–8%), both muscles had low-level concentric activity, presumably as a small co-contraction to the highly active tibialis anterior. Both muscles lengthened before push-off as the leg rotated forward over the foot, which was flat on the ground and absorbed energy from the leg. Both SOL and MG reached peak activity at 45–50% of stride during the high powered push-off period when the ankle underwent rapid plantarflexion, indicating a rapid generation of energy to propel the limb upward and forward. During early swing (65–80% of stride), both SOL and MG had low-level eccentric activity as a co-contraction to the TA, which was rapidly shortening to cause the foot to dorsiflex for toe clearance. The remainder of SOL and MG activity was low for the balance of swing and appeared to be a continued co-contraction to the TA.

TA activity (Fig. 7) peaked at 6% and showed a lengthening action from 0 to 6% as the foot was eccentrically lowered from its flexed and supinated position to the ground. Then, once the foot was flat on the ground, this muscle remained active until 20% and was observed to shorten, thus pulling the leg forward over the foot. Because the increasing eccentric action of the much larger plantarflexors has already been noted, the TA activity also appears to be co-contraction to the dominant plantarflexors. Although such co-contractions are inefficient, the ankle joint probably is being stabilized during this transition from dorsiflexor to plantar-

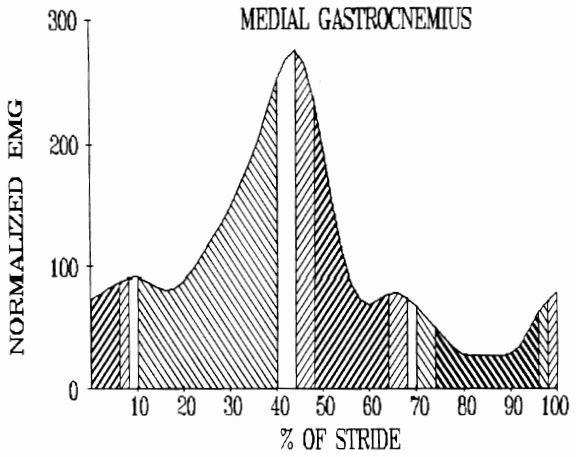


**FIG. 6.** Linear envelope electromyography profile of medial gastrocnemius shaded to indicate concentric and eccentric functions. Shading is as described in legend to Fig. 5.

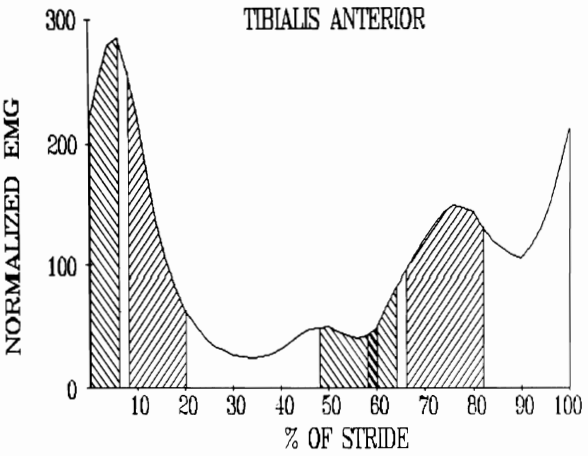


**FIG. 7.** Linear envelope electromyography profile of tibialis anterior shaded to indicate concentric and eccentric activity. Shading is as described in legend to Fig. 5.

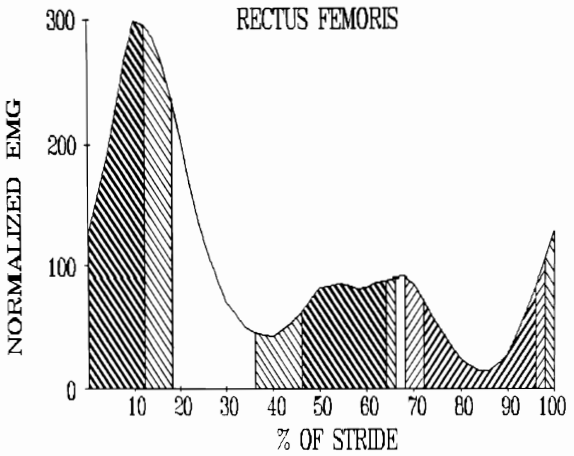


**FIG. 9.** Linear envelope electromyography profile of rectus femoris shaded to show concentric and eccentric activity. Shading is as described in legend to Fig. 5.

flexor activity. Then, during midstance, the TA has low-level activity and is essentially isometric. During late stance (and early swing) TA acts to provide a low-level co-contraction to the rapidly shortening plantarflexors. Then, until early swing, TA increases activity as it shortens rapidly to dorsiflex the foot. For the balance of swing, TA has high-level and increasing activity that holds the foot isometrically against gravity and the plantarflexors in preparation for HC.

VL and RF (Figs. 8 and 9) have similar LE profiles, but some functional differences exist because RF also crosses the hip joint. During weight acceptance when the knee is flexing (0–15%), both muscles reach peak activity in an eccentric contraction, but RF lengthens more rapidly because it is also

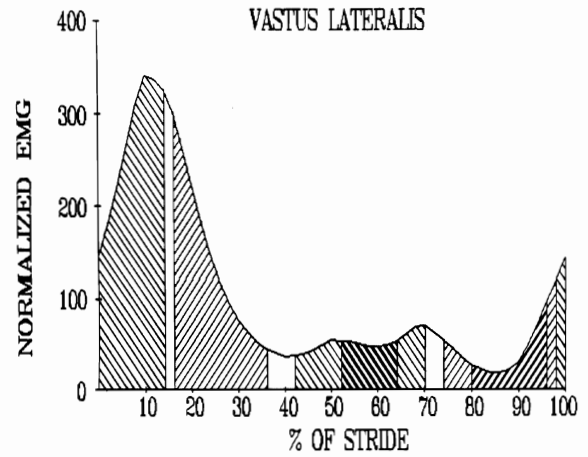


**FIG. 8.** Linear envelope electromyography profile of vastus lateralis shaded to show concentric and eccentric functions. Shading is as described in legend to Fig. 5.

lengthening at its origin as the hip extends. Then during midstance (15–40%) the knee extends and VL concentrically contracts to increase the potential energy of the body. However, the RF during most of this time (18–36%) has no net shortening; it lengthens at its origin and shortens at the knee. During push-off and early swing (40–70% of stride), the knee flexes quite rapidly and this dominates the function of both muscles; both absorb energy in an eccentric contraction to control the amount of knee flexion during this rapid unloading phase. For the balance of swing, both muscles have low-level concentric activity as the knee rapidly extends. This activity does not dominate because the net knee moment during this period is flexor (13); thus, this quadriceps activity is a co-contraction to the dominant hamstrings. The profile of the representative hamstring, ST, is shown in Fig. 10. Its peak activity occurs just before HC but has a high and decreasing level during weight acceptance and midstance. As explained with respect to Fig. 4, during all of stance this muscle is shortening and therefore is generating energy. Such a shortening will act to extend the hip, causing the thigh to rotate forward, thus providing some extra forward propulsion from the rear. This generation of energy has been noted in mechanical power analyses as positive hip power, mainly early in stance (13).

This hip energy-generating mechanism is accentuated in certain pathologies, especially when ankle push-off power is impaired; e.g., below-the-knee amputees generate above-normal hip extensor power early in stance (15). During most of swing, ST is lengthening as the knee extends and EMG

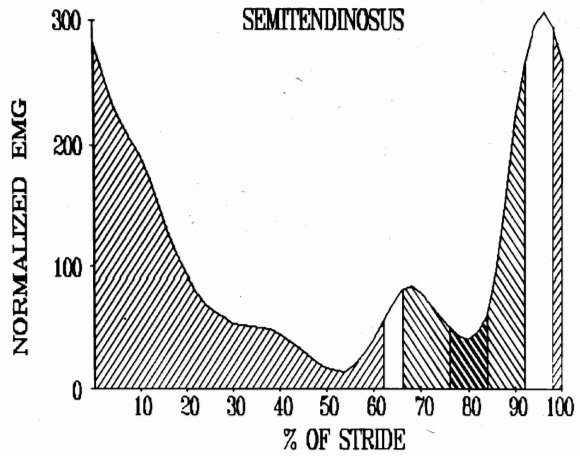


**FIG. 10.** Linear envelope electromyography profile of semitendinosus shaded to show concentric and eccentric function. Shading is as described in legend to Fig. 5.

activity increases rapidly; kinetic energy is removed from the leg and foot before HC. Just before HC, the hamstrings actually shorten for a very short period to reverse the direction of the foot so as to reduce the forward velocity of the heel to near-zero just before HC. Such short bursts of activity have been noted in mechanical power analyses of runners at times when it is extremely critical for them to reduce forward velocity of the heel to near-zero before HC (11).

## CONCLUSION

Our techniques allow researchers and clinicians to process EMG signals using LE to produce a tension-related profile. Easily accessible joint angle data combined with readily available computer graphics permit the LE to be colored or shaded to enable further interpretation regarding the role of each muscle as a generator or absorber of mechanical energy.

**Acknowledgment:** We thank Paul Guy for technical assistance. This work was supported by Grant No. MT4343 from the Medical Research Council of Canada.

## REFERENCES

1. Calvert TW, Chapman AE: Relationship between surface EMG and force transients in muscle: simulation and experimental results. *Proc IEEE* 65:682–689, 1977.
2. Dostal WF, Andrews JG: A three-dimensional biomechanical model of hip musculature. *J Biomech* 14:803–812, 1981.
3. Inman VT, Ralston HJ, Saunders JBde, Feinstein B, Wright EW Jr: Relation of human electromyogram to muscle tension. *Electroencephalogr Clin Neurophysiol* 4:187–194, 1952.
4. Kadaba MP, Wootten ME, Gainey J, Cochran GVB: Repeatability of phasic muscle activity: performance of surface and intramuscular wire electrodes in gait analysis. *J Orthop Res* 3:330–359, 1985.
5. Komi PV, Buskirk ER: Reproducibility of electromyographic measurements with inserted wire electrodes and surface electrodes. *Electromyography* 4:357–367, 1970.
6. Milner-Brown HS, Stein RB, Yemm R: Contractile properties of human motor units during voluntary isometric contractions. *J Physiol* 228:285–306, 1973.
7. Olney SJ, Winter DA: Predictions of knee and ankle moments in walking from EMG and kinematic data. *J Biomech* 18:9–20, 1985.
8. Pierrynowski MR, Morrison JB: Estimating the muscle forces generated in the human lower extremity when walking: a physiological solution. *Math Biosci* 75:43–68, 1985.
9. Scott SH, Winter DA: A comparison of three muscle pinnation assumptions and their effect on isometric and isotonic force. *J Biomech* 24:163–167, 1991.
10. White SC, Yack HJ, Winter DA: A three-dimensional musculoskeletal model for gait analysis: anatomical variability estimates. *J Biomech* 22:885–893, 1989.
11. Winter DA: Moments of force and mechanical power in slow jogging. *J Biomech* 16:91–97, 1983.
12. Winter DA: Pathological gait diagnosis with computer-averaged electromyographic profiles. *Arch Phys Med Rehabil* 65:393–398, 1984.
13. Winter DA: *Biomechanics and motor control of human gait.* University of Waterloo Press, Waterloo, Ontario, 1987.
14. Winter DA, Yack HJ: EMG profiles during normal human walking: stride-to-stride and intersubject variability. *Electroencephalogr Clin Neurophysiol* 67:402–411, 1987.
15. Winter DA, Sienko SE: Biomechanics of below-knee amputee gait. *J Biomech* 21:361–367, 1988.
16. Yang JF, Winter DA: EMG amplitude normalization methods: on improving its sensitivity as a diagnostic tool in gait analysis. *Arch Phys Med Rehabil* 65:517–521, 1984.